Contributions of excitation autoionization to electron-impact ionization of Mg-like Al^+, S^{4+}, Cl^{5+}, and Ar^{6+} ions

S. S. Tayal and Ronald J. W. Henry
Department of Physics and Astronomy, Louisiana State University, Baton Rouge, Louisiana 70803-4001
(Received 27 January 1986)

The R-matrix method is used to calculate the contributions of excitation autoionization to electron-impact ionization in Mg-like Al^+, S^{4+}, Cl^{5+}, and Ar^{6+} ions. The ground $3s^2\,{}^1S$ state together with the autoionizing states arising from the $2p^5 3s^2 3p$, $2p^5 3s^2 3d$, $2p^5 3s^2 4s$, $2s\,2p^6 3s^2 3p$, $2s\,2p^6 3s^2 3d$, and $2s\,2p^6 3s^2 4s$ configurations are included in the R-matrix expansion. Large numbers of bound terms of appropriate symmetry are included in the expansion to account for the resonant-excitation—double-autoionization process. The total ionization cross sections are obtained by combining the cross sections for inner-shell excitation with direct-ionization cross sections. Our calculation shows an abrupt and significant rise in the cross sections, in agreement with recent crossed-beam measurements of Howald *et al.* The importance of indirect processes over the direct process increases with increasing ionic charge along the sequence.

I. INTRODUCTION

The electron-impact-ionization cross sections and rates for positive ions are of fundamental importance in the analysis of high-temperature, low-density astrophysical and laboratory plasmas.[1,2] In the case of complex positive ions a number of physical mechanisms can contribute to the ionization cross sections. For example, in the direct-ionization process either a valence electron or any of the inner subshell electrons are knocked out from the ion by electron impact. Alternatively, the ionization process can proceed by electron-impact excitation of an inner subshell electron to a quasibound state lying in the continuum, followed by autoionization.[3] The latter process is the dominant mechanism for electron-impact ionization of some highly ionized atoms close to threshold and its significance increases with increasing ionic charge along the isoelectronic sequence. In addition to excitation autoionization, there is another possible indirect process contributing to electron-impact ionization in which the incident electron is captured into a compound state of the target plus incident electron followed by double autoionization.[4] Such resonances occur as Rydberg series below each of the excited states. The excitation-autoionization effects cause a sharp rise in the ionization cross sections at threshold energies.

In the past, there have been many experimental and theoretical activities in this area. On the theoretical side, most of the predictions have relied upon semiempirical formulas and scaling laws.[5] The semiempirical formula due to Seaton[6] has been used for the cross sections close to the threshold region while the more widely used Lotz formula[7] has been employed for the direct electron-impact ionization cross sections well above the threshold region. According to the Lotz formula the cross section σ (in cm^2) at a collision energy E is given by

$$\sigma(E)=4.5\times10^{-14}\sum_j \frac{r_j}{I_j E}\ln(E/I_j)\ , \tag{1}$$

where r_j is the number of electrons in subshell j, and I_j is the ionization energy for electrons of that subshell. The energies are expressed in eV.

Recently, Burgess and Chidichimo[8] have suggested a semiempirical formula, which in addition to the direct ionization, allows for indirect processes such as inner-shell excitation autoionization. Several theoretical calculations have been carried out using quantum-mechanical methods such as Coulomb-Born, distorted-wave, Coulomb-Born-exchange, and distorted-wave-exchange[9,10] for various isoelectronic sequences and for many specific ions. For Li-like and Be-like ions, Jakubowicz and Moores[11] have carried out Coulomb-Born-exchange and distorted-wave-exchange calculations using close-coupling wave functions to represent the initial and final states of the ions. Golden and Sampson[12] have given a method for scaling the Coulomb-Born-exchange calculations for hydrogenic ions in the limit $Z\rightarrow\infty$ to other ions.

The significant contribution from excitation autoionization has been accounted for by adding the relevant excitation cross sections obtained in a close-coupling approximation to the direct-ionization cross sections for a number of ions of Li and Na sequences by Henry,[13] Henry and Msezane,[14] and Crandall *et al.*[15] A similar procedure was adopted by Burke and co-workers to calculate electron-impact ionization cross sections of Ca^+ and Ti^{3+} using the R-matrix method.[16,17] Our concern here is with similar calculations on Mg-like ions: Al^+, S^{4+}, Cl^{5+}, and Ar^{6+}. The crossed-beam experimental data has very recently become available for these ions.[18–20] These types of *ab initio* calculations are very difficult to perform as there may be an infinite number of strongly coupled final states. Therefore, in order to make the calculations tractable one is forced to include a finite number of well-chosen excited autoionizing states in the close-coupling expansion. In our calculations we include excitation-autoionization reactions of the type where a $2p$ electron is first excited into a $3p$, $3d$, or $4s$ orbital;

$$e^- + x^{q+}(1s^2 2s^2 2p^6 3s^2)\rightarrow x^{q+*}(1s^2 2s^2 2p^5 3s^2 nl)+e^-\ , \tag{2}$$

followed by the autoionization process

$$x^{q+*}(1s^2 2s^2 2p^5 3s^2 nl) \rightarrow x^{(q+1)+}(1s^2 2s^2 2p^6 3s) + e^- , \tag{3}$$

and also, where a $2s$ electron is first excited into a $3p$, $3d$, or $4s$ orbital:

$$e^- + x^{q+}(1s^2 2s^2 2p^6 3s^2) \rightarrow q^{q+*}(1s^2 2s\, 2p^6 3s^2 nl) + e^- , \tag{4}$$

followed by the autoionization process

$$x^{q+*}(1s^2 2s 2p^6 3s^2 nl) \rightarrow x^{(q+1)+}(1s^2 2s^2 2p^6 3s) + e^- . \tag{5}$$

In Sec. II we describe the wave functions and present the details of our R-matrix calculations. The results are presented in Sec. III, where they are discussed and compared with the recent experimental data and other theoretical predictions.

II. THEORY

A. Target wave functions

We have included the $3s^2\,{}^1S$ ground state together with the excited autoionizing states corresponding to the $2p^5 3s^2 3p$, $2p^5 3s^2 3d$, $2p^5 3s^2 4s$, $2s\,2p^6 3s^2 3p$, $2s\,2p^6 3s^2 3d$, and $2s\,2p^6 3s^2 4s$ configurations in our calculations. As discussed before, there are many other possible autoionizing states which may contribute to the excitation-autoionization cross sections. However, to keep our calculations manageable we included these 20 autoionizing states (14 for Al^+), and we believe that these would give the most important contribution to the excitation-autoionization cross sections. In a test run on Al^+, the excited $3s\,3p\,{}^{1,3}P^\circ$ states were also included. It was found that the coupled channels due to these states do not have any appreciable effect on the inner-shell excitation cross sections. Therefore, we did not include these states in our calculation on other ions. The ground state of the ion was represented by configuration interaction (CI) expansion containing $3s^2$, $3p^2$, $3d^2$, $2p^5 3s^2 3p$, and $2s\,2p^6 3s^2 4s$ configurations, while for the excited states the CI expansion was limited to the states included in the close-coupling expansion. We used seven orthogonal one-electron orbitals: $1s$, $2s$, $2p$, $3s$, $3p$, $3d$, and $4s$. The $1s$, $2s$, $2p$, and $3s$ radial functions are those of the $3s^2\,{}^1S$ ground state given by Clementi and Roetti.[21] The $3p$, $3d$, and $4s$ radial functions were obtained with computer program CIV3 (Ref. 22) on minimizing the energies of the $2p^5 3s^2 3p\,{}^1P$, $2p^5 3s^2 3d\,{}^1P^\circ$, and $2p^5 3s^2 4s\,{}^1P^\circ$ states, respectively. Each of these orbitals was expanded in Slater-type orbitals of the form[23]

$$P_{nl}(r) = \sum_i C_i r^{p_i} \exp(-\xi_i r) . \tag{6}$$

In Table I we give the parameters of the Slater-type orbitals for the non-Hartree-Fock functions. The coefficients C_i are uniquely determined by the orthonormality conditions. In Table II the excitation energies in eV relative to the ground state are presented. The excitation energies are found to scale approximately as $(Z-9)^{3/2}$ along the isoelectronic sequence.

B. Continuum wave function

The wave function representing the electron-ion collision is expanded as

$$\Psi_k = \mathcal{A} \sum_{i,j} \Phi_i(1,2,\ldots,N;\hat{r}_{N+1}\sigma_{N+1}) r_{N+1}^{-1} u_{ij}(r_{N+1}) a_{ijk} + \sum_j \phi_j(1,2,\ldots,N+1) b_{jk} , \tag{7}$$

where $\mathcal{A}$ is the antisymmetrization operator, $1,2,\ldots,N+1$ represent the space and spin coordinates of the $N+1$ electrons in the system, the Φ_i are channel functions consisting of wave functions for the target coupled with spin and angular functions for the scattered electron, and u_{ij} are the numerical basis functions describing the radial motion of the scattered electron. These are obtained by solving the zero-order radial differential equation

$$\left[\frac{d^2}{dr^2} - \frac{l_i(l_i+1)}{r^2} + V(r) + k_j^2\right] u_{ij}(r) = \sum_k \lambda_{ijk} P_k(r) \tag{8}$$

satisfying the boundary conditions

$$u_{ij}(0) = 0 , \qquad \frac{a}{u_{ij}(a)} \frac{du_{ij}}{dr}\bigg|_{r=a} = b . \tag{9}$$

$V(r)$ is a zero-order potential which is chosen to be the ground-state static potential, b is a constant which we

TABLE I. Values of Slater-type orbital parameters.

Orbital	P_i	ξ_i Al^+	S^{4+}	Cl^{5+}	Ar^{6+}
$3p$	2	5.035 04	6.396 51	6.846 85	7.294 52
	3	1.424 87	2.384 79	2.700 64	3.016 47
$3d$	3	0.928 30	2.071 36	2.433 66	2.792 04
$4s$	1	10.563 34	12.620 22	1.698 15	13.976 41
	2	4.236 40	5.276 10	7.923 85	5.932 56
	3	1.788 55	2.541 61	5.518 76	3.028 51
	4	0.906 93	1.680 85	1.928 60	2.193 58

TABLE II. Excitation energies (eV) of the autoionizing states relative to the ground state.

State	Al^+	S^{4+}	Cl^{5+}	Ar^{6+}
$1s^22s^22p^53s^23p\ ^3S$	78.76	173.39	212.61	255.65
^3D	79.62	175.10	214.59	257.91
^1D	80.11	176.10	215.75	259.23
^3P	80.19	176.24	215.92	259.41
^1P	80.19	176.24	215.92	259.41
^1S	84.95	185.47	226.53	271.41
$1s^22s^22p^53s^23d\ ^3P^\circ$	88.27	195.94	238.80	285.37
$^3F^\circ$	89.39	196.37	239.37	286.08
$^1F^\circ$	89.42	196.73	239.88	286.76
$^3D^\circ$	89.54	197.15	240.39	287.35
$^1D^\circ$	89.54	197.15	240.39	287.35
$^1P^\circ$	89.51	198.19	242.05	289.71
$1s^22s^22p^53s^24s\ ^3P^\circ$	88.27	207.17	257.19	312.38
$^1P^\circ$	88.69	207.62	257.71	312.96
$1s^22s\,2p^63s^23p\ ^3P^\circ$		239.03	294.35	343.67
$^1P^\circ$		240.08	295.60	345.03
$1s^22s\,2p^63s^23d\ ^3D$		259.95	318.72	371.38
^1D		260.49	319.53	372.49
$1s^22s\,2p^63s^24s\ ^3S$		270.64	336.39	397.48
^1S		271.68	347.82	409.13

have taken as zero, and a is the radius of the sphere defining the internal region. The Lagrange undetermined multipliers λ_{ijk} ensure that the continuum orbitals are orthogonal to bound orbitals with the same angular symmetry.

The coefficient a_{ijk} and b_{jk} are determined by diagonalizing the total Hamiltonian of the electron-plus-ion system in the basis defined by (7). The details of the R-matrix method can be found in Burke and Robb.[24]

In order to account for the process in which the incident electron is captured into a compound state of target ion plus incident electron, we have included a large number of bound terms ϕ_j of the appropriate symmetry in the second expansion in Eq. (7). A zero logarithmic derivative was imposed at the boundary $a=15.2$, 8.8, 6.9, and 6.8 a.u. on the continuum basis orbitals for Al^+, S^{4+}, Cl^{5+}, and Ar^{6+}, respectively.

Twenty-five continuum orbitals of each angular symmetry were included, giving good convergence in the energy ranges considered in this work. The R matrix was calculated on the boundary $r=a$ using the R-matrix computer package of Berrington *et al.*[25] For the study of excitation autoionization we are interested in the transitions of the type $3s^2\,^1S\rightarrow 2p^53s^23p\ ^{1,3}S$, $^{1,3}P$, $^{1,3}D$, $2p^53s^23d\ ^{1,3}P^\circ$, $^{1,3}D^\circ$, $^{1,3}F^\circ$, $2p^53s^24s\ ^{1,3}P^\circ$, $2s\,2p^63s^23p\ ^{1,3}P^\circ$, $2s\,2p^63s^23d\ ^{1,3}D$, and $2s\,2p^63s^24s\ ^{1,3}S$ followed by decay by autoionization. The total cross section is the sum of the excitation cross sections for all these transitions. It has been assumed that all the excited autoionizing states do in fact autoionize. At each electron energy results were obtained for nine values of angular momenta $L=0$ to 8. These partial waves gave converged cross sections for forbidden and spin-changing transitions. However, for electric dipole allowed transitions, $3s^2\,^1S\rightarrow 2p^53s^23d\ ^1P^\circ$ and $3s^2\,^1S\rightarrow 2p^53s^24s\ ^1P^\circ$, the convergence could not be achieved with nine partial waves. The contribution from higher partial waves ($L>8$) for these transitions was obtained using the close-coupling program NIEM.[26]

The coupled differential equations were solved in the outer region ($r>a$) to yield the S matrix and hence the cross sections. In the evaluation of the coupled differential equations, we ignored the long-range potential coefficients. This approximation reduces the problem to the evaluation of Coulomb functions on the R-matrix boundary. The Coulomb functions for open and closed channels were obtained using the computer program of Barnet *et al.*[27] and Bell and Scott,[28] respectively. This method has the advantage of being computationally much faster and its accuracy was tested by Tayal *et al.*[29] and Dufton and Kingston[30] for Al^+ and S^{4+}, respectively. Their test calculations showed that this did not lead to significant errors.

III. RESULTS AND DISCUSSION

We calculated the total ionization cross sections using the relation[3]

$$\sigma_{\text{total}}=\sigma_{\text{direct}}+\sum_j \sigma^j_{\text{excit}}B^a_j\ , \tag{10}$$

where $\sigma_{\text{direct}}$is the direct-ionization cross section, σ^j_{excit} is the excitation cross section to the j autoionizing state, and B^a_j is the branching ratio for autoionization from the level j which is assumed to be unity in the present work. The

direct-ionization cross sections have been obtained from the Lotz semiempirical formula[7] and from distorted-wave calculations using Younger's parameters.[31] The Lotz formula overestimates the cross sections compared to distorted-wave results. Distorted-wave results for direct-ionization cross sections are in better agreement with the shape of the experimental data[19] before the onset of indirect processes. Similar agreement was obtained between experiment and Younger's distorted-wave predictions for the Li- and Na-like ions.[15,32] Therefore, Younger's distorted-wave results are chosen to represent the direct-ionization contribution to the total ionization cross sections. However, it should be noted that Younger's direct-ionization cross sections for Ar^{6+} are about 15% less than the experimental data before the onset of indirect processes. These results for Ar^{6+} are scaled to the other members of the sequence using the experimental ionization potentials of the ions.

We have included a large number of autoionizing states in our calculations. These states are believed to give the most important contribution to the excitation-autoionization cross sections. These states represent excitations of the type $2p \rightarrow 3p,3d$ and $2s \rightarrow 3p,3d$ ($\Delta n=1$); and $2p \rightarrow 4s$ and $2s \rightarrow 4s$ ($\Delta n=2$). The notation $2p \rightarrow 3p,3d,4s$ represent excitations shown by Eq. (2), while $2s \rightarrow 3p,3d,4s$ excitations are represented by Eq. (4). The excitation-autoionization features associated with higher excited states with $\Delta n \geq 2$ are expected to be very small as the excitations scale approximately as n^{-3}. We have listed the cross sections for inner-shell excitation of four ions of the Mg-isoelectronic sequence as a function of electron energy k^2 (in Ry) in Tables III and IV. The collision strengths Ω which are related to the cross sections σ by the relation

$$\Omega=\omega k^2\sigma \ , \tag{11}$$

where ω is the statistical weight of the initial state, show the expected large energy behavior. For the forbidden $2p \rightarrow 3p$ transitions, the collision strength is approximately constant with increasing energy, while they increase as $\ln E$ for the optically allowed $2p \rightarrow 3d$ and $2p \rightarrow 4s$ transitions.

The results of our calculation for the electron-impact ionization cross section of Al^+ are shown in Fig. 1, where they are compared with the recent experimental data of Montague and Harrison[18] and Belic *et al.*[20] In both experiments, the Al^+ ion beam contained some percentage of metastable ions. Montague and Harrison have estimated 9% metastable ions in their experiment and have corrected the measured data for their presence. We have plotted their derived ground-state cross sections in the figure. The measurements of Montague and Harrison are lower than the Belic *et al.* results at energies larger than 40 eV. A part of the difference is perhaps due to the fact that one has been corrected for the presence of metastable ions while the other still contains contributions from them. We have also shown the semiempirical estimates of

TABLE III. Excitation cross sections (10^{-18} cm^2).

Ion	k^2	$2p \rightarrow 3p$	$2p \rightarrow 3d+4s$	$2s \rightarrow 3p+3d+4s$	Total
Al^+	6.0	2.52			2.52
	6.3	2.35			2.35
	6.5	2.98			2.98
	6.6	3.20	0.67		3.87
	7.0	3.27	0.82		4.09
	7.5	3.40	0.76		4.16
	8.0	3.31	0.72		4.03
	10.0	2.75	0.62		3.37
	12.5	2.24	0.59		2.83
	16.0	1.73	0.56		2.29
	18.5	1.44	0.53		1.97
	22.0	1.15	0.52		1.67
Ion	k^2	$2p \rightarrow 3p$	$2p \rightarrow 3d+4s$	$2s \rightarrow 3p+3d+4s$	Total
S^{4+}	13.9	1.04			1.04
	14.0	1.49			1.49
	14.6	1.42	0.55		1.97
	15.0	1.38	0.52		1.90
	15.5	1.33	0.94		2.27
	16.0	1.28	0.92		2.20
	18.0	1.14	0.84		1.98
	20.0	1.02	0.80	0.18	2.00
	25.0	0.79	0.72	0.33	1.84
	30.0	0.65	0.67	0.29	1.61
	35.0	0.55	0.65	0.25	1.45
	40.0	0.46	0.64	0.23	1.33
	45.0	0.40	0.62	0.22	1.24

TABLE IV. Excitation cross sections (10^{-18} cm^2).

Ion	k^2	$2p \rightarrow 3p$	$2p \rightarrow 3d + 4s$	$2s \rightarrow 3p + 3d + 4s$	Total
Cl^{5+}	16.7	1.08			1.08
	17.5	1.03			1.03
	17.8	1.02	0.82		1.84
	18.0	1.00	0.82		1.82
	18.5	0.97	0.83		1.80
	19.0	0.94	0.81		1.75
	20.0	0.89	0.78		1.67
	25.0	0.71	0.68		1.39
	30.0	0.57	0.60	0.25	1.42
	35.0	0.48	0.57	0.23	1.28
	40.0	0.41	0.60	0.19	1.20
	45.0	0.36	0.59	0.18	1.13
	50.0	0.32	0.58	0.17	1.07
	60.0	0.26	0.55	0.15	0.96
	70.0	0.22	0.52	0.14	0.88
Ar^{6+}	20.0	0.79			0.79
	22.0	0.72	0.78		1.50
	22.9	0.68	1.11		1.79
	24.0	0.65	0.67		1.32
	25.0	0.62	0.66		1.28
	30.0	0.51	0.59		1.10
	35.0	0.43	0.53	0.22	1.18
	40.0	0.37	0.50	0.18	1.05
	45.0	0.33	0.49	0.15	0.97
	50.0	0.29	0.48	0.14	0.91
	60.0	0.24	0.46	0.12	0.82
	70.0	0.20	0.44	0.11	0.75

direct-ionization cross sections given by the Lotz formula[7] [Eq. (1)] and the distorted-wave direct-ionization cross sections obtained by using Younger's parameters.[31] The Lotz formula overestimates the cross sections beyond 30 eV. The peak of our excitation autoionization cross section occurs at about 102 eV, where the value is 4.16×10^{-18} cm^2 (see Table III). The highest energy which we could consider in our R-matrix calculation is 300 eV. The $2p \rightarrow 3p$ transitions give the largest contribution to the excitation-autoionization cross sections over

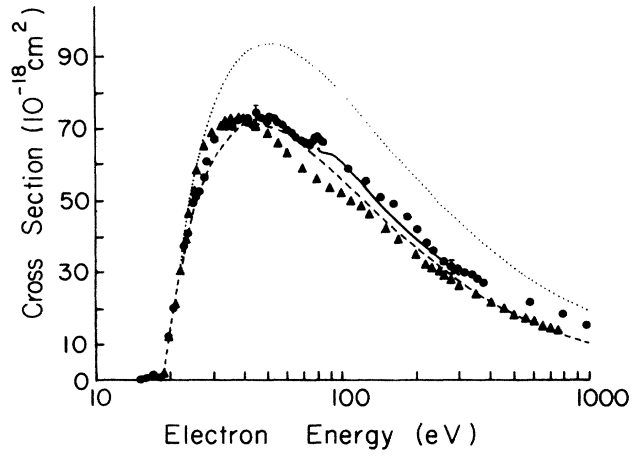

FIG. 1. Electron-impact-ionization cross section for the ground $3s^2\,{}^1S$ state of Al^+. Solid triangles, experimental data of Montague and Harrison (Ref. 18); solid circles, measured cross sections of Belic *et al.* (Ref. 20); — — —, distorted-wave cross section for direct ionization using Younger's parameters (Ref. 31); . . . ., semiempirical formula of Lotz (Ref. 7) for direct ionization; ——, present calculations for excitation autoionization plus distorted-wave cross section for direct ionization.

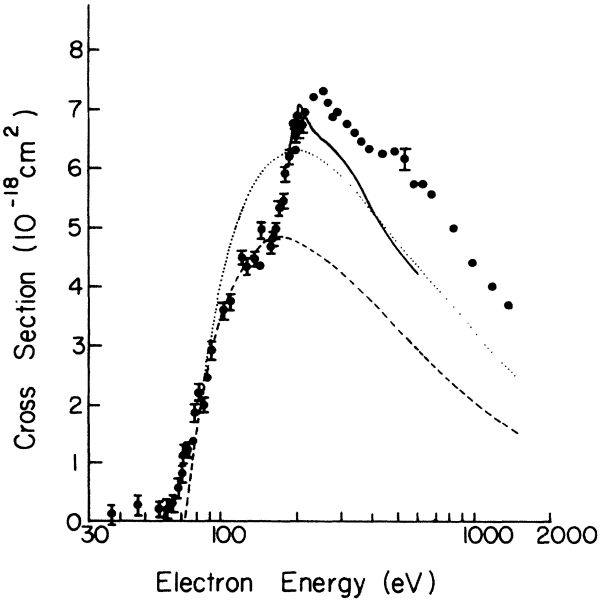

FIG. 2. Electron-impact-ionization cross section for the ground $3s^2\,{}^1S$ state of S^{4+}. Solid circles, experimental results of Howald *et al.* (Ref. 19). Other notations as in Fig. 1.

the entire energy region.

Electron-impact-ionization cross sections for S^{4+}, Cl^{5+}, and Ar^{6+} are given in Figs. 2, 3, and 4, respectively. The results of present calculations given by Eq. (10) are shown by solid lines. The dashed curves give the distorted-wave direct-ionization cross sections,[31] while the results of the Lotz formula[7] are shown by dotted curves. The crossed-beam experimental data of Howald *et al.*[19] are shown by solid circles. The onset of the ionization cross sections at energies below the ground-state thresholds indicates the presence of metastable ions in the ion beams. The experimental results show a sharp rise in the cross sections close to thresholds which clearly indicates the importance of indirect processes such as excitation autoionization for these ions. Similar jumps in the cross section at threshold were observed for ions of Li and Na sequences and several other ions, and a detailed discussion on the significance of excitation autoionization is given in Crandall,[1] Crandall *et al.*,[15] and Falk *et al.*[33]

Our calculations predict an abrupt rise in cross sections at approximately the correct energy. The peaks of our calculated cross sections are lower in height and lie about 50 eV towards the lower-energy side. The peak values of excitation-autoionization cross sections are 2.27×10^{-18}, 1.84×10^{-18}, and 1.79×10^{-18} cm^2, as is evident from Table III, and these occur at electron energies 210, 242, and 312 eV for the S^{4+}, Cl^{5+}, and Ar^{6+} ions, respectively. The highest energies which we could consider in our R-matrix calculations for these ions are, respectively, 45, 70, and 75 Ry. The relative importance of different types of transitions to the excitation-autoionization cross sections can be easily seen from Tables III and IV. The relative contributions of $2p\rightarrow3p$ and $2p\rightarrow3d+4s$ change as Z increases. At Al^+, $2p\rightarrow3p$ dominates [the ratio of $\Omega(2p\rightarrow3p)$ to $\Omega(2p\rightarrow3d+4s)$ is 3.6 at $x=2$, where $x=k^2/\Delta E$], whereas the ratio decreases with increasing Z to 1.0, 0.82, and 0.73 at $x=2$ for S^{4+}, Cl^{5+}, and Ar^{6+}, respectively. As the energy increases, all values of the ratio decrease since $2p\rightarrow3d+4s$ is an allowed process which behaves as $\ln x$ for large x, whereas $2p\rightarrow3p$ is forbidden and is approximately constant with energy.

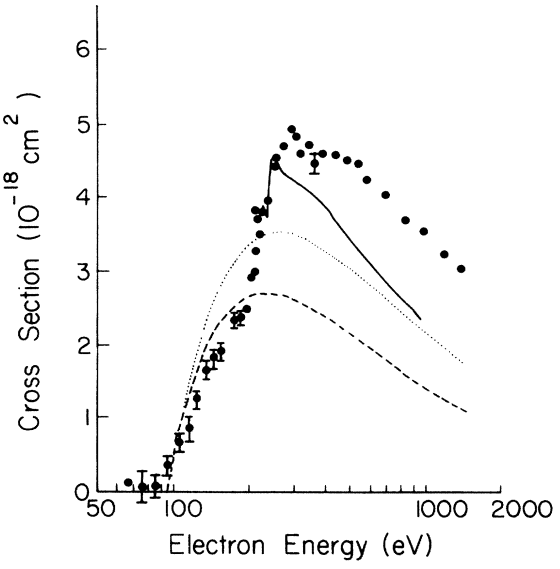

FIG. 3. Electron-impact-ionization cross section for the ground $3s^2\,{}^1S$ state of Cl^{5+}. Notations as in Fig. 2.

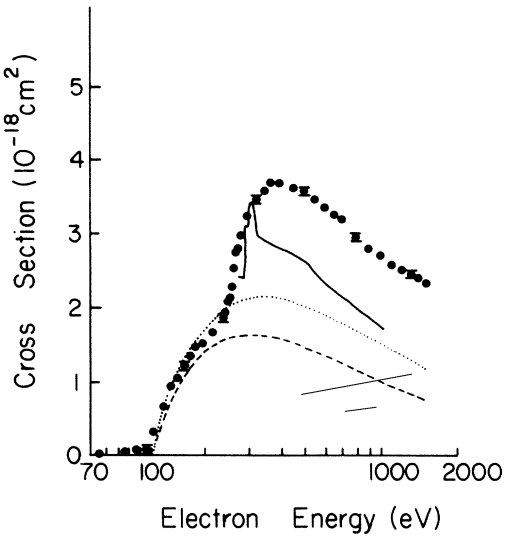

FIG. 4. Electron-impact-ionization cross section for the ground $3s^2\,{}^1S$ state of Ar^{6+}. Notations as in Fig. 2.

Pindzola *et al.*[34] have very recently calculated the excitation-autoionization cross sections for the Mg-like S^{4+}, Cl^{5+}, and Ar^{6+} ions in the distorted-wave approximation. Our results for $2p\rightarrow3p$ excitation cross sections close to threshold energies are 1.49×10^{-18}, 1.08×10^{-18}, and 0.79×10^{-18} cm^2 for S^{4+}, Cl^{5+}, and Ar^{6+}, respectively, which are in excellent agreement with the 1.43×10^{-18}, 1.04×10^{-18}, and 0.76×10^{-18} cm^2 distorted-wave results. However, for $2p\rightarrow3d$ excitations, the distorted-wave results 1.47×10^{-18}, 1.23×10^{-18}, and 1.01×10^{-18} cm^2 are larger compared to the present close-coupling results 0.87×10^{-18}, 0.79×10^{-18}, and 0.77×10^{-18} cm^2 for S^{4+}, Cl^{5+}, and Ar^{6+}, respectively. The difference may be attributed to the strong-coupling and configuration-interaction effects. The magnitude of the off-diagonal terms in the reactance matrix decreases with the increasing ionic charge along the sequence. However, the magnitude remains appreciable even for Ar^{6+} indicating the strong-coupling effects between the states. Because of the important coupling effects present in many ions, particularly for the lower members of the isoelectronic sequences, the distorted-wave calculations overestimate the cross sections for the inner-shell excitation-autoionization compared to close-coupling approximations.[14,16]

Resonance structure is evident for lower energies, where some of the calculations are made at energies insufficient to excite all states included in the expansion. No attempt has been made to systematically study this structure, but its presence explains the peculiar shape of the cross sections for energies less than 90, 210, 260, and 315 eV for Al^+, S^{4+}, Cl^{5+}, and Ar^{6+}, respectively. At high energies the present results are lower compared to experimental data. This disagreement is perhaps partly due to the presence of significant metastable ions in the experiment and partly due to the various approximations which we have

made in our calculations. For example, we have not considered the quantum-mechanical interference which may arise between various contributing processes, and we have neglected the finite width of the autoionizing states and assumed the excited states to be purely bound. Howald *et al.*[9] have argued that the slow falloff of their cross sections at higher energies is due to the substantial metastable ions which will lead to the inner-shell direct ionization of $2p$ electrons contributing to the single ionization in their measurements. This is supported by the distorted-wave cross-section calculations of Pindzola *et al.*[34] We have not considered the cross sections from metastable $2p^6 3s\,3p$ levels in the present calculations.

IV. CONCLUSIONS

In this paper we have described the calculation of indirect processes to ionization cross sections for magnesiumlike Al^+, S^{4+}, Cl^{5+}, and Ar^{6+} ions. The experimental data for these ions have recently become available. We have seen that the excitation autoionization gives substantial contributions to the cross sections, in agreement with the experiment. However, the presence of large metastable content in the target beam makes the comparison of our results with the experimental data rather difficult.

The ratios of the indirect cross section to the direct cross section at the peak for Al^+, S^{4+}, Cl^{5+}, and Ar^{6+} are 0.075, 0.49, 0.69, and 1.1, respectively, which clearly indicates the increasing importance of the indirect processes with increasing Z along the Mg-isoelectronic sequence. We have neglected the interference between direct ionization and excitation autoionization, and the importance of this effect for magnesiumlike ions is not known. However, Crandall *et al.*[15] have argued that this interference effect did not make an appreciable contribution for O^{5+}. Finally, for higher members of the sequence the radiative decay may compete with the autoionization and an allowance should be made to account for the radiative process for highly ionized ions.

ACKNOWLEDGMENTS

This work was supported in part by the U.S. Department of Energy (Division of Chemical Sciences). We are grateful to G. H. Dunn, D. C. Gregory, and M. S. Pindzola for communicating their results prior to publication.

[1]D. H. Crandall, Phys. Scr. **23**, 153 (1981).
[2]R. D. Cowan and J. B. Mann, Astrophys. J. **232**, 940 (1979).
[3]O. Bely, J. Phys. B **1**, 23 (1968); L. Goldberg, A. K. Duprees, and J. W. Allen, Annu. Rev. Astron. Astrophys. **28**, 589 (1965).
[4]K. J. LaGattuta and Y. Hahn, Phys. Rev. A **24**, 2273 (1981).
[5]E. J. McGuire, Phys. Rev. A **16**, 73 (1977).
[6]M. J. Seaton, Planet. Space Sci. **12**, 55 (1964).
[7]W. Lotz, Z. Phys. **216**, 241 (1968).
[8]A. Burgess and M. C. Chidichimo, Mon. Not. R. Astron. Soc. **203**, 1269 (1983).
[9]D. C. Griffin, C. Bottcher, and M. S. Pindzola, Phys. Rev. A **25**, 154 (1982).
[10]D. C. Griffin, C. Bottcher, and M. S. Pindzola, Phys. Rev. A **25**, 1374 (1972).
[11]H. Jakubowicz and D. L. Moores, J. Phys. B **14**, 3733 (1981).
[12]L. B. Golden and D. H. Sampson, J. Phys. B **10**, 2229 (1977).
[13]R. J. W. Henry, J. Phys. B **12**, L309 (1979).
[14]R. J. W. Henry and A. Z. Msezne, Phys. Rev. A **26**, 2545 (1982).
[15]D. H. Crandall, R. A. Phaneuf, D. C. Gregory, A. M. Howald, D. W. Mueller, T. S. Morgan, G. H. Dunn, and R. J. W. Henry, Phys. Rev. A (to be published).
[16]P. G. Burke, A. E. Kingston, and A. Thomas, J. Phys. B **16**, L385 (1983).
[17]P. G. Burke, W. C. Fon, and A. E. Kingston, J. Phys. B **17**, L733 (1984).
[18]R. G. Montague and M. F. A. Harrison, J. Phys. B **16**, 3045 (1983).
[19]A. M. Howald, D. C. Gregory, F. W. Meyer, R. A. Phaneuf, A. Muller, N. Djuric, and G. H. Dunn, Phys. Rev. A **33**, 3780 (1986), this issue.
[20]D. S. Belic, R. A. Falk, C. Timmer, and G. H. Dunn (private communication).
[21]E. Clementi and C. Roetti, At. Data Nucl. Data Tables **14**, 177 (1974).
[22]A. Hibbert, Comput. Phys. Commun. **9**, 141 (1975).
[23]S. S. Tayal and A. Hibbert, J. Phys. B **17**, 3835 (1984).
[24]P. G. Burke and W. D. Robb, Adv. At. Mol. Phys. **11**, 143 (1975).
[25]K. A. Berrington, P. G. Burke, M. Le Dourneuf, W. D. Robb, K. T. Taylor, and Vo Ky Lan, Comput. Phys. Commun. **14**, 367 (1978).
[26]R. J. W. Henry, S. P. Rountree, and E. R. Smith, Comput. Phys. Commun. **23**, 233 (1981).
[27]A. R. Barnet, D. H. Feng, J. W. Steed, and L. J. B. Goldfarb, Comput. Phys. Commun. **8**, 377 (1974).
[28]K. L. Bell and N. S. Scott, Comput. Phys. Commun. **20**, 447 (1980).
[29]S. S. Tayal, P. G. Burke, and A. E. Kingston, J. Phys. B **17**, 3847 (1984).
[30]P. L. Dufton and A. E. Kingston, J. Phys. B **17**, 3321 (1984).
[31]S. M. Younger, *Atomic Data for Fusion,* edited by D. H. Crandall, C. F. Barnett, and W. L. Wiese (Controlled Fusion Atomic Data Center, Oak Ridge National Laboratory, Oak Ridge, Tenn., 1981), Vol. 7, p. 190.
[32]D. H. Crandall, R. A. Phaneuf, R. A. Falk, D. S. Belic, and G. H. Dunn, Phys. Rev. A **25**, 143 (1982).
[33]R. A. Falk, G. H. Dunn, D. C. Griffin, C. Bottcher, D. C. Gregory, D. H. Crandall, and M. S. Pindzola, Phys. Rev. Lett. **47**, 494 (1981).
[34]M. S. Pindzola, D. C. Griffin, and C. Bottcher, Phys. Rev. A **33**, 3788 (1986), this issue.